Classical critical behavior of spin models with long-range interactions

Erik Luijten* and Henk W. J. Blöte
Department of Physics, Delft University of Technology, Lorentzweg 1, 2628 CJ Delft, The Netherlands
(Received 2 April 1997)

We present the results of extensive Monte Carlo simulations of Ising models with algebraically decaying ferromagnetic interactions in the regime where classical critical behavior is expected for these systems. We corroborate the values for the exponents predicted by renormalization theory for systems in one, two, and three dimensions and accurately observe the predicted logarithmic corrections at the upper critical dimension. We give both theoretical and numerical evidence that above the upper critical dimension the decay of the critical spin-spin correlation function in finite systems consists of two different regimes. For one-dimensional systems our estimates for the critical couplings are more than two orders of magnitude more accurate than existing estimates. In two and three dimensions we are unaware of any other results for the critical couplings. [S0163-1829(97)05638-5]

I. INTRODUCTION

The critical behavior of Ising models with long-range interactions has attracted much attention during the last three decades. For the one-dimensional case, some analytical results have been obtained,[1–11] as well as a number of numerical results. The numerical results apply to both inverse-square interactions[12–15] and general algebraically decaying interactions.[16–27] The work by Anderson, Yuval, and Hamann,[28–31] which greatly stimulated the interest in spin chains with long-range interactions, deserves special mention. They also developed a renormalizationlike approach to the one-dimensional (1D) inverse-square model.[30,31] Further renormalization-group studies of this particular case are presented in Refs. 12 and 32–34. A major contribution was made by Fisher, Ma, and Nickel[35] and Sak,[36] who obtained renormalization predictions for the critical exponents of models of general dimensionality $d<4$ with algebraically decaying interactions (obtained independently by Suzuki *et al.*[37]). Other works concerning $d>1$ are two conjectures on, respectively, the boundary between long-range and short-range behavior and the boundary between classical (mean-field) and nonclassical behavior, both by Stell,[38] a (refuted) conjecture by Griffiths,[39] a rigorous confirmation of the upper critical dimension by Aizenman and Fernández,[10] and a variational approach to the Ising model with long-range interactions.[40] Furthermore, Monte Carlo simulations have been carried out for one particular choice of the spin-spin interaction in a two-dimensional model.[41] However, to our knowledge, neither any further verifications of the renormalization predictions nor any other results are available for higher-dimensional ($d>1$) models. To conclude this summary, we mention that the one-dimensional q-state Potts model with long-range interactions has been studied analytically,[9,11] numerically,[42,43] and in a mean-field approximation on the Bethe lattice.[44]

Why are these models interesting? In the first place from a fundamental point of view: They enable us to study the influence of the interaction range on the critical behavior. For example, in one-dimensional systems long-range order is only possible in the presence of spin–spin interactions which decay sufficiently slowly. In the borderline (inverse-square) case, the 1D model displays a remarkable behavior: At the critical temperature the order parameter exhibits a finite jump (see Sec. II), but the free energy has an essential singularity such that all thermal properties are smooth. In this sense, the phase transition can be regarded as the one-dimensional analog of a Kosterlitz-Thouless transition,[45,46] although the jump in the magnetization is not present there, as follows from the Mermin-Wagner theorem.[47] Just as $d=2$ is the lower critical dimension for the two-dimensional XY model with short-range interactions, $\sigma=1$ is a critical decay rate in a one-dimensional system with interactions decaying as $r^{-(1+\sigma)}$, see Ref. 32. With respect to higher-dimensional systems, we note that the decay rate of van der Waals forces in realistic three-dimensional systems is only slightly faster than at the boundary between short-range (Ising-like) and long-range critical behavior. The question of criticality in ionic systems, where the (screened) Coulomb interactions might lead to effectively algebraically decaying interactions, appears still open to debate.[48–50] It has also been claimed that exponents in the long-range universality class have been observed experimentally in a ferromagnetic phase transition.[51] Recently, it has been derived that critical fluctuations may give rise to long-range Casimir forces (decaying much more slowly than van der Waals interactions) between uncharged particles immersed in a critical fluid.[52] Furthermore, it was shown by Anderson and Yuval[28,29] that the Kondo problem corresponds to a one-dimensional Ising model with a combination of inverse-square and nearest-neighbor interactions. Yet another application follows from Ref. 22, where it was shown that random exchange (Lévy-flight) processes can generate effective interactions which decay algebraically. Hence, the universal critical properties of the nonequilibrium steady state of these systems are those of the long-range equilibrium Ising models studied in this paper. Finally, the realization that the upper critical dimension can be varied by tuning the decay rate of the interaction led to a special application of these models in Ref. 53. Here, they were used to analyze a long-standing controversy on the universality of the renormalized coupling constant above the upper critical dimension.

In this article, we present accurate numerical results for Ising systems with algebraically decaying interactions in one, two, and three dimensions. Until now, the long-range character of the spin-spin interactions has been the main bottleneck for the examination of these systems by means of numerical methods (and, in fact, also for their analytical solution). All previously published numerical results therefore rely on various extrapolations based on data for small systems. However, the development of a more powerful Monte Carlo algorithm[54] enabled us to efficiently simulate these systems. The high accuracy of the results opens several perspectives: (i) verification of the renormalization predictions for the critical exponents; (ii) accurate observation of logarithmic corrections at the upper critical dimension; (iii) first estimates of the critical temperatures of two- and three-dimensional systems with long-range interactions; (iv) verification of previously obtained estimates of the critical temperatures of one-dimensional systems, which in addition implies a check on the various extrapolation methods that have been developed; (v) verification of predicted bounds on the critical temperatures; (vi) verification of a conjecture on the behavior of the critical temperature as a function of the decay parameter. Another problem one encounters in the simulations is the large parameter space: The simulations for a set of different temperatures and system sizes have to be repeated for a range of values of the decay parameter and for $d=1,2,3$. The total computing time dedicated to the results presented in this paper amounts to approximately two CPU years on a modern workstation. Part of the numerical results presented in this work have been reported in concise form in Ref. 53.

The outline of this paper is as follows. In Sec. II, we sum up the known rigorous results for the Ising chain with long-range interactions. In Sec. III, we review the renormalization scenario of these models and derive the finite-size scaling behavior of several quantities. This includes the corrections to scaling, both at and above the upper critical dimension. Our numerical results are presented and analyzed in Sec. IV and compared with previously obtained results. Finally, we summarize our conclusions in Sec. V. The Appendix contains technical details concerning the application of the long-range Monte Carlo algorithm to the models studied in this paper.

II. RIGOROUS RESULTS FOR THE ONE-DIMENSIONAL CASE

For the one-dimensional case, the Hamiltonian is given by

$$\mathcal{H}=\sum_{ij} J(i-j)s_i s_j, \tag{1}$$

where the sum runs over all spin pairs. We are particularly interested in algebraically decaying interactions, i.e., $J(n) \propto n^{-\alpha}$. To ensure that the energy of the system does not diverge, it is required that $\alpha>1$. In 1968, Ruelle[1] rigorously proved the absence of long-range order in a spin chain with ferromagnetic spin-spin couplings $J(i-j)$ such that the sum

$$\sum_{n=1}^{N} nJ(n) \tag{2}$$

does not diverge in the limit $N\to\infty$. For algebraically decaying interactions, this implies the absence of a phase transition for $\alpha>2$. Shortly later, Dyson[2] proved the *existence* of a phase transition if the sums $\Sigma_{n=1}^{N} J(n)$ and $\Sigma_{n=1}^{N} (\ln\ln n)[n^3 J(n)]^{-1}$ both converge, for positive and monotonically decreasing $J(n)$. In particular, a phase transition occurs for $J(n)\propto n^{-\alpha}$ with $1<\alpha<2$. This *partly* corroborated the conjecture of Kac and Thompson,[55] viz., that there is a phase transition for $1<\alpha\leqslant 2$. Furthermore, Dyson[3] was (as were—much later—also Rogers and Thompson[6]) able to replace Ruelle's condition with a stronger one, which however still left the case $\alpha=2$ undecided. This also holds for an even more stringent criterion by Thouless,[4] who generalized the argument of Landau and Lifshitz[56] for the absence of a phase transition in an Ising chain with short-range interactions. However, Thouless argued on entropic grounds that *if* a phase transition exists for $\alpha=2$, the magnetization must have a *discontinuity* at the transition point. This was later dubbed the ''Thouless effect'' by Dyson, who proved it to occur in the closely related hierarchical model.[57] Simon and Sokal made Thouless' argument partially rigorous,[5] but later Aizenman *et al.*[9] showed that, although a discontinuity in the order parameter *is indeed present* if there is a phase transition, his argument does *not* account for this. Namely, Thouless had assumed that the spin-spin correlation function $\langle s_0 s_r\rangle - \langle s_0\rangle\langle s_r\rangle$ vanishes in the limit $r\to\infty$, whereas actually the critical exponent η is equal to 1 in this case. Meanwhile, Fröhlich and Spencer[7] had been able to rigorously prove the *existence* of a phase transition in the borderline case and thus to corroborate the Kac-Thompson conjecture for $\alpha=2$ as well. Another interesting point is the rigorous proof for the existence of an intermediate ordered phase in the one-dimensional model with inverse-square interactions, where the two-point correlation function exhibits power-law decay with an exponent that varies continuously in a finite temperature range below the critical temperature.[11]

III. FINITE-SIZE ANALYSIS OF THE CRITICAL BEHAVIOR

Already in a very early stage of the history of the ε expansion, Fisher, Ma, and Nickel analyzed the critical behavior of d-dimensional systems ($d<4$) with long-range interactions decaying as $r^{-(d+\sigma)}$, with $\sigma>0$.[35] They concluded that the upper critical dimension is given by $d_u=2\sigma$, as was previously conjectured by Stell[38] and later rigorously proven by Aizenman and Fernández.[10] For more slowly decaying interactions, $0<\sigma<d/2$, the critical behavior is classical, whereas the critical exponents assume nonclassical, continuously varying values for $d/2<\sigma<2$. For $\sigma>2$ they take their short-range values. Sak,[36] however, found that already for $\sigma>2-\eta_{sr}$ the critical behavior is Isinglike, where η_{sr} denotes the exponent η in the corresponding model with short-range interactions. In this article we concentrate on the classical range, for which we have performed extensive Monte Carlo simulations of spin models in $d=1,2,3$. The nonclassical range will be the subject of a future article.[58]

We briefly outline the renormalization scenario for these models, in order to derive the finite-size scaling relations required to analyze the numerical data. We start from the

following Landau-Ginzburg-Wilson Hamiltonian in momentum space,

$$\mathcal{H}(\phi_{\mathbf{k}})/k_{\mathrm{B}}T=\frac{1}{2}\sum_{\mathbf{k}}\ (j_{\sigma}k^{\sigma}+j_{2}k^{2}+r_{0})\phi_{\mathbf{k}}\phi_{-\mathbf{k}} +\frac{u}{4N}\sum_{\mathbf{k}_1}\sum_{\mathbf{k}_2}\sum_{\mathbf{k}_3}\ \phi_{\mathbf{k}_1}\phi_{\mathbf{k}_2}\phi_{\mathbf{k}_3}\phi_{-\mathbf{k}_1-\mathbf{k}_2-\mathbf{k}_3} -h\sqrt{\frac{N}{2}}\phi_{\mathbf{k}=\mathbf{0}}. \tag{3}$$

The $j_{\sigma}k^{\sigma}$ term arises from the Fourier transform of the interactions decaying as $r^{-(d+\sigma)}$. The j_2k^2 term normally representing the short-range interactions is included because it will appear anyway in the renormalization process and will compete with the long-range term.[36] Under a renormalization transformation with a rescaling factor $b=e^{l}$, the term $j_{\sigma}k^{\sigma}$ is transformed into $j_{\sigma}k'^{\sigma}$, with $\mathbf{k}'=\mathbf{k}b$. To keep the coefficient of the k^{σ} term fixed, we rescale the field $\phi_{\mathbf{k}}$ to $\phi'_{\mathbf{k}'}=b^{-\sigma/2}\phi_{\mathbf{k}}$. Thus, the coefficient of the k^2 term decreases as $b^{\sigma-2}$ and the coefficient of the ϕ^4 term changes proportional to $b^{2\sigma-d}$. Hence, the Gaussian fixed point dominates the renormalization flow for $\sigma<d/2$, which is the situation studied in this paper.

For the sake of generality we treat here the case of an n-component order parameter with $O(n)$ symmetry. The renormalization equations are then given by

$$\frac{dr_0}{dl}=\sigma r_0+a(n+2)u(c-r_0), \tag{4a}$$

$$\frac{du}{dl}=\varepsilon u-a(n+8)u^2, \tag{4b}$$

where $(n+2)$ and $(n+8)$ are the usual factors arising from the tensorial structure of the interaction part of the Hamiltonian and $\varepsilon=2\sigma-d$. These equations are not complete to second order, because the $\mathcal{O}(u^2)$ term is missing in Eq. (4a).

We first consider the case $\varepsilon<0$. The solution of the second equation is given by

$$u(l)=\overline{u}e^{\varepsilon l}\frac{1}{1+\overline{u}[a(n+8)/\varepsilon](e^{\varepsilon l}-1)}, \tag{5}$$

where $\overline{u}$ denotes the value of u at $l=0$. This yields, to leading order in u, the following solution for the first equation:

$$r_0(l)=[\overline{r}_0+ac(n+2)\overline{u}/(d-\sigma)]\times e^{\sigma l}\left[\frac{1}{1+[a(n+8)/\varepsilon]\overline{u}(e^{\varepsilon l}-1)}\right]^{(n+2)/(n+8)} -\frac{ac(n+2)\overline{u}e^{\varepsilon l}/(d-\sigma)}{1+[a(n+8)/\varepsilon]\overline{u}(e^{\varepsilon l}-1)}, \tag{6}$$

with $\overline{r}_0\equiv r_0(l=0)$. The first factor between square brackets is proportional to the reduced temperature $t\equiv(T-T_c)/T_c$ and the last term is the so-called shift of the critical temperature. The factors $[1+a(n+8)\overline{u}(e^{\varepsilon l}-1)/\varepsilon]^{-1}$ in Eqs. (5) and (6) are higher-order corrections in u. Under successive renormalization transformations, u approaches the value $u^*=0$ and the Gaussian fixed point (0,0) is thus indeed stable. The pertinent renormalization exponents are: $y_t=\sigma$, $y_h=(d+\sigma)/2$, and $y_i=2\sigma-d$.

At $\varepsilon=0$, the Gaussian fixed point becomes marginally stable. Solving Eq. (4b) leads to

$$u^{\mathrm{uc}}(l)=\frac{\overline{u}}{1+a(n+8)\overline{u}\,\overline{l}}, \tag{7}$$

where the superscript ''uc'' indicates that we are operating at the upper critical dimension. This solution can be used to solve, again to leading order in u, Eq. (4a), yielding

$$r_0^{\mathrm{uc}}(l)=[\overline{r}_0+ac(n+2)\overline{u}/(d/2)]\times e^{\sigma l}\left[\frac{1}{1+a(n+8)\overline{u}\,\overline{l}}\right]^{(n+2)/(n+8)} -\frac{ac(n+2)\overline{u}/(d/2)}{1+a(n+8)\overline{u}\,\overline{l}} \tag{8}$$

or, in terms of the rescaling factor b,

$$r_0^{\mathrm{uc}}=[\overline{r}_0+ac(n+2)\overline{u}/(d/2)]\times b^{\sigma}\left[\frac{1}{1+a(n+8)\overline{u}\ln b}\right]^{(n+2)/(n+8)} -\frac{ac(n+2)\overline{u}/(d/2)}{1+a(n+8)\overline{u}\ln b}. \tag{9}$$

Since σ is fixed at $d/2$ the factor $d/2$ in the last term is identical to the corresponding factor $(d-\sigma)$ in Eq. (6). Further comparison of Eqs. (6) and (8) shows that above the upper critical dimension the leading shift of the critical temperature is proportional to b^{ε}, whereas this factor vanishes at the upper critical dimension itself and the factor $(e^{\varepsilon l}-1)/\varepsilon$ in the second-order term turns into a $\ln b$ term, yielding a logarithmic shift of the form $1/(A\ln b+B)$.

From the solutions of the renormalization equations we can derive the scaling behavior of the free energy and of (combinations of) its derivatives. For the case $\varepsilon<0$ the free-energy density f scales, to leading order, as

$$f(t,h,u,1/L)=b^{-d}f(b^{y_t}[t+\tilde{\alpha}ub^{y_i-y_t}],b^{y_h}h,b^{y_i}u,b/L)+g, \tag{10}$$

where $\tilde{\alpha}=-ac(n+2)/(d-\sigma)$ and we have included a finite-size field L^{-1}. g denotes the analytic part of the transformation. We abbreviate the first term on the right-hand side as $b^{-d}f(t',h',u',b/L)$. However, we must take into account the fact that, for $T\leqslant T_c$, the free energy is singular at $u=0$. This makes u a so-called *dangerous* irrelevant variable; see, e.g., Ref. 59. As discussed in Ref. 53, the correct finite-size scaling properties are obtained by setting $b=L$

and making the substitution $\phi' = \phi/u'^{1/4}$. This leads to a new universal function, $\tilde{f}$, with

$$f(t',h',u',1) + \overline{g} = \tilde{f}(\tilde{t},\tilde{h}), \tag{11}$$

where $\tilde{t} = t'/u'^{1/2}$ and $\tilde{h} = h'/u'^{1/4}$. The analytic part of the transformation also contributes to the singular dependence of the free energy on t (see, e.g., Ref. 60, Chap. VI, Sec. 3): Despite the regularity of this term in each single renormalization step, the infinite number of steps still leads to the buildup of a singularity. This contribution, denoted by $\overline{g}$, is absorbed in $\tilde{f}$ as well. Setting $b = L$ and combining Eqs. (10) and (11) yields

$$f\left(t,h,u,\frac{1}{L}\right) = L^{-d}\tilde{f}\left(L^{y_t - y_i/2}\frac{1}{u^{1/2}}[t + \tilde{\alpha}uL^{y_i - y_t}], L^{y_h - y_i/4}\frac{h}{u^{1/4}}\right) \tag{12a}$$

$$= L^{-d}\tilde{f}\left(L^{y_t^*}\frac{1}{u^{1/2}}[t + \tilde{\alpha}uL^{y_i - y_t}], L^{y_h^*}\frac{h}{u^{1/4}}\right). \tag{12b}$$

Here, we have introduced the exponents $y_t^* \equiv y_t - y_i/2 = d/2$ and $y_h^* \equiv y_h - y_i/4 = 3d/4$. The corresponding critical exponents indeed assume their fixed, classical values; $\alpha = 0$, $\beta = 1/2$, $\gamma = 1$, $\delta = 3$. The exponent γ is singled out here as a special case; even without taking into account the modification of y_t and y_h due to the dangerous irrelevant variable one obtains the classical value $\gamma = 1$. Since the correlation length exponent $\nu = 1/y_t$ (it is not affected by the singular dependence of the free energy on u), we see that hyperscaling is violated, which is a well-known result for systems above their upper critical dimension.[59] The rescaling of the pair-correlation function $g(\mathbf{r})$ (decaying proportional to $1/r^{d-2+\eta}$) relates the exponent η to the rescaling factor of the field, yielding $\eta = 2 - \sigma$. Note that this contrasts with the short-range case ($\sigma = 2$), where η assumes its mean-field value for all dimensionalities $d \geqslant 4$. This implies that direct experimental measurement of either ν or η offers a way to discern whether the interactions in a system are mean-field-like ($\nu = 1/2$, $\eta = 0$) or have the form of a slowly decaying power law. *Below* the upper critical dimension, however, the finite-size scaling behavior of the spin-spin correlation function is (apart from a volume factor) identical to that of the magnetic susceptibility χ. This relation yields a contradiction above the upper critical dimension, since χ depends on the scaled combination $tL^{y_t^*}$, instead of tL^{y_t}. Indeed, the susceptibility diverges as $t^{-\gamma}$ and the finite-size behavior of χ is thus $\chi_L \propto L^{\gamma y_t^*} = L^{d/2}$, corresponding to $g_L \propto L^{-d/2}$. On the other hand, if one assumes that the finite-size behavior of the correlation function is identical to its large-distance behavior, one expects that $g_L \propto L^{-(d-2+\eta)} = L^{-(d-\sigma)}$. Only at the upper critical dimension, $d_u = 2\sigma$, these two predictions coincide. We will return to this point at the end of this section. Furthermore, we will examine the behavior of the spin-spin correlation function in Sec. IV.

At the upper critical dimension itself, i.e., at $\varepsilon = 0$, the free-energy density scales as

$$f\left(t,h,u,\frac{1}{L}\right) = b^{-d}f\left(\frac{b^{y_t}}{(1+\tilde{\beta}u\ln b)^{(n+2)/(n+8)}} \times \left[t + \tilde{\alpha}b^{-y_t}\frac{u}{(1+\tilde{\beta}u\ln b)^{6/(n+8)}}\right], b^{y_h}h, \frac{u}{1+\tilde{\beta}u\ln b}, \frac{b}{L}\right) + g \tag{13a}$$

$$= L^{-d}\tilde{f}\left(\frac{L^{y_t}}{(1+\tilde{\beta}u\ln L)^{(n+2)/(n+8)-1/2}}\frac{1}{u^{1/2}} \times \left[t + \tilde{\alpha}L^{-y_t}\frac{u}{(1+\tilde{\beta}u\ln L)^{6/(n+8)}}\right], L^{y_h}\frac{h}{u^{1/4}}[1+\tilde{\beta}u\ln L]^{1/4}\right), \tag{13b}$$

where $\tilde{\beta} = a(n+8)$ and we have set $b = L$ in the last line. u is now a marginal variable and although we again have to perform the substitution $\phi \to \phi'$ (the Gaussian fixed point is marginally stable), the exponents y_t and y_h coincide with y_t^* and y_h^*, respectively, because y_i vanishes. Thus, the scaling relations (12b) and (13b) differ to leading order only in the logarithmic factors arising in the arguments of $\tilde{f}$.

As usual, the finite-size scaling relations are now found by taking derivatives of the free-energy density with respect to the appropriate scaling fields. In the Monte Carlo simulations we have sampled the second and the fourth moment of the magnetization density, the dimensionless amplitude ratio $Q \equiv \langle m^2\rangle^2/\langle m^4\rangle$ (which is directly related to the Binder cumulant[61]), and the spin-spin correlation function over half the system size (for even system sizes). The second moment of the magnetization density is (apart from a volume factor) equal to the second derivative of the free-energy density with respect to h,

$$\langle m^2\rangle = L^{-d}\frac{\partial^2 f}{\partial h^2}(t,h,u,1/L) = L^{2y_h^* - 2d}u^{-1/2} \times \tilde{f}^{(2)}\left(L^{y_t^*}\frac{\hat{t}}{u^{1/2}}, L^{y_h^*}\frac{h}{u^{1/4}}\right), \tag{14}$$

where $\tilde{f}^{(2)}$ stands for the second derivative of $\tilde{f}$ with respect to its second argument and $\hat{t} \equiv t + \tilde{\alpha}uL^{y_i - y_t}$. At $\varepsilon = 0$, logarithmic factors do arise not only in the arguments of $\tilde{f}^{(2)}$, but also in the prefactor,

$$\langle m^2\rangle = L^{2y_h-2d}\left(\frac{1+\tilde{\beta}u\ln L}{u}\right)^{1/2} \times \tilde{f}^{(2)}\left(\frac{L^{y_t}}{(1+\tilde{\beta}u\ln L)^{(n+2)/(n+8)-1/2}}\frac{1}{u^{1/2}} \times\left[t+\tilde{\alpha}L^{-y_t}\frac{u}{(1+\tilde{\beta}u\ln L)^{6/(n+8)}}\right], L^{y_h}\frac{h}{u^{1/4}}[1+\tilde{\beta}u\ln L]^{1/4}\right). \quad (15)$$

For the fourth magnetization moment similar expressions hold and in the amplitude ratio Q all prefactors divide out, both for $\varepsilon<0$ and $\varepsilon=0$. Thus we find that the ratio Q is given by a universal function $\tilde{Q}$,

$$Q_L(T)=\tilde{Q}\left(L^{y_t^*}\frac{\hat{t}}{u^{1/2}}\right)+q_1L^{d-2y_h^*}+\cdots, \quad (16)$$

where we have omitted the h dependence of $\tilde{Q}$, since we are only interested in the case $h=0$. The additional term proportional to q_1 arises from the h dependence of the analytic part of the free energy[62] and the ellipsis stands for higher powers of $L^{d-2y_h^*}$ (faster-decaying terms). At $\varepsilon=0$, $\hat{t}$ must be replaced by the first argument within square brackets in Eq. (13b), multiplied by the factor $(1+\tilde{\beta}u\ln L)^{1/2-(n+2)/(n+8)}$. Finally, we may derive the finite-size scaling behavior of the spin-spin correlation function $g(\mathbf{r})$ by differentiating the free-energy density to two *local* magnetic fields, which couple to the spins at positions $\mathbf{0}$ and $\mathbf{r}$, respectively, and assuming that the finite-size behavior is identical to the r dependence of g. If we do not take into account the dangerous irrelevant variable mechanism, we find $g_L \propto L^{2y_h-2d}=L^{-(d-\sigma)}$, just as we found before from $\eta=2-\sigma$. However, replacing y_h by y_h^* yields $g_L\propto L^{-d/2}$, in agreement with the L dependence of the magnetic susceptibility. This clarifies the difference between the two predictions: At short distances (large wave vectors), the $j_\sigma k^\sigma \phi_{\mathbf{k}}\phi_{-\mathbf{k}}$ term will be the dominant term in the Landau-Ginzburg-Wilson Hamiltonian and there is no ''dangerous'' dependence on u. Hence, the finite-size behavior of the spin-spin correlation function will be given by $L^{-(d-2+\eta)}$. For $\mathbf{k}=\mathbf{0}$, the coefficient of the ϕ^2 term vanishes and thus the $u\phi^4$ term is required to act as a bound on the magnetization. To account for this singular dependence on u, we rescale the field, which implies that y_h is replaced by y_h^* and g_L scales as $L^{2y_h^*-2d}$. In a finite system, the wave vectors assume discrete values, $\mathbf{k}=(n_x,n_y,n_z)2\pi/L$, and thus it is easily seen that even for the lowest nonzero wave vectors $j_\sigma k^\sigma \phi_{\mathbf{k}}\phi_{-\mathbf{k}}$ constitutes the dominant bounding term on the magnetization. Namely, the coefficient of the ϕ^4 term contains a volume factor L^{-d} [cf. Eq. (3)] and this term is thus (above the upper critical dimension) a higher-order contribution decaying as $L^{2\sigma-d}$.

IV. NUMERICAL RESULTS AND COMPARISON WITH EARLIER RESULTS

A. Simulations

We have carried out Monte Carlo simulations for systems described by the Hamiltonian

$$\mathcal{H}/k_BT=-\sum_{\langle ij\rangle}J(|\mathbf{r}_i-\mathbf{r}_j|)s_is_j, \quad (17)$$

where the sum runs over all spin pairs and periodic boundaries were employed. The precise form of the (long-range) spin-spin interaction $J(r)$ as used in the simulations was chosen dependent on the dimensionality. For $d=1$ we have followed the conventional choice $J(r)=K/r^{d+\sigma}$ (with *discrete* values for r), as this allows us to compare *all* our results (including nonuniversal quantities) to previous estimates. However, as explained in Ref. 54 and the Appendix, this discrete form requires the construction of a lookup table, which becomes inefficient for higher dimensionalities. For $d=2$ we have thus applied an interaction which is the integral of a continuously decaying function,

$$J(|\mathbf{r}|)=K\int_{r_x-1/2}^{r_x+1/2}dx\int_{r_y-1/2}^{r_y+1/2}dy(x^2+y^2)^{-(d+\sigma)/2}, \quad (18)$$

where $\mathbf{r}=(r_x,r_y)$. In $d=3$ the corresponding volume integral was used for $J|\mathbf{r}|$. This modification of the interaction does only change nonuniversal quantities like the critical temperature, but should not influence the universal critical properties like the critical exponents and dimensionless amplitude ratios, since the difference between the continuous and the discrete interaction consists of faster decaying terms that are irrelevant according to renormalization theory. Details concerning the simulations can be found in the Appendix.

The following system sizes have been examined: chains of length $10\leqslant L\leqslant 150\,000$, square systems of linear size $4\leqslant L\leqslant 240$, and cubic systems of linear size $4\leqslant L\leqslant 64$. At the upper critical dimension simulations for even larger systems have been carried out in order to obtain accurate results from the analyses: $L=300\,000$ in $d=1$ and $L=400$ in $d=2$. (I.e., in terms of numbers of particles the largest system size for $d=2$ is considerably smaller than for $d=1$ and $d=3$.) For the simulations we used a new cluster algorithm for long-range interactions.[54] This algorithm is $\mathcal{O}(L^{d+z})$ times faster than a conventional Metropolis algorithm, where z is the dynamical critical exponent. For systems displaying mean-field-like critical behavior, we expect an exponent $d/2$ instead of z and the efficiency gain in our simulations is thus of the order of 10^8 for the largest system sizes. For each data point we have generated between 10^6 and 4×10^6 Wolff clusters.

B. Determination of the critical temperatures, the amplitude ratio Q, and the thermal exponent

The critical couplings K_c of these systems have been determined using an analysis of the amplitude ratio Q. The finite-size scaling analysis was based on the Taylor expansion of Eq. (16), which for $\varepsilon<0$ reads

TABLE I. The amplitude ratio Q and the thermal exponent y_t^* for systems with long-range interactions in one, two, and three dimensions, for several values of the decay parameter $0<\sigma\leqslant d/2$. The values in the fifth column have been obtained with Q fixed at the theoretically predicted value (see text) and the last column lists the renormalization predictions for y_t^*.

d	σ	Q	y_t^*	y_t^*	RG
1	0.1	0.4566 (8)	0.507 (7)	0.507 (7)	$\frac{1}{2}$
1	0.2	0.455 (4)	0.54 (4)	0.504 (12)	$\frac{1}{2}$
1	0.25	0.457 (3)	0.500 (8)	0.500 (5)	$\frac{1}{2}$
1	0.3	0.454 (2)	0.519 (14)	0.506 (12)	$\frac{1}{2}$
1	0.4	0.457 (3)	0.50 (2)	0.50 (2)	$\frac{1}{2}$
1	0.5	0.462 (6)	0.51 (5)	0.49 (2)	$\frac{1}{2}$
2	0.2	0.4574 (10)	1.01 (2)	1.01 (2)	1
2	0.4	0.455 (2)	1.02 (2)	1.009 (15)	1
2	0.6	0.450 (6)	1.04 (4)	1.008 (17)	1
2	0.8	0.454 (6)	1.03 (9)	1.03 (3)	1
2	1.0	0.450 (10)	1.02 (3)	1.03 (2)	1
3	0.2	0.4581 (11)	1.51 (3)	1.513 (18)	$\frac{3}{2}$
3	0.4	0.4561 (10)	1.521 (18)	1.512 (15)	$\frac{3}{2}$
3	0.6	0.453 (3)	1.53 (4)	1.521 (14)	$\frac{3}{2}$
3	0.8	0.458 (2)	1.48 (2)	1.487 (10)	$\frac{3}{2}$
3	1.0	0.453 (10)	1.52 (7)	1.508 (9)	$\frac{3}{2}$
3	1.2	0.447 (8)	1.56 (2)	1.519 (10)	$\frac{3}{2}$
3	1.4	0.454 (5)	1.48 (3)	1.48 (3)	$\frac{3}{2}$
3	1.5	0.449 (8)	1.53 (5)	1.46 (3)	$\frac{3}{2}$

$$Q_L(T)=Q+p_1\hat{t}L^{y_t^*}+p_2\hat{t}^2L^{2y_t^*}+p_3\hat{t}^3L^{3y_t}+\cdots+q_1L^{d-2y_h^*}+\cdots+q_3L^{y_i}+\cdots. \tag{19}$$

The term proportional to $\tilde{\alpha}$ in $\hat{t}$ yields a contribution $q_2L^{y_i/2}=q_2L^{\sigma-d/2}$ and the term $q_3L^{y_i}$ comes from the denominator in Eq. (5). The coefficients p_i and q_i are nonuniversal. In addition to the corrections to scaling in Eq. (19) we have also included higher powers of $q_3L^{y_i}$, which become particularly important when y_i is small (i.e., when σ is close to $d/2$), higher powers of $q_1L^{d-2y_h^*}=q_1L^{-d/2}$, and the cross-term proportional to $L^{y_t^*+y_i}$.

All analyses were carried out on the same data set as used in Ref. 53, to which several data points have been added for most values of σ. First, we have only kept fixed the exponents in the correction terms, y_i and y_h^*. The corresponding estimates for Q and y_t^* are shown in the third and fourth column of Table I. One observes that the Monte Carlo results for both Q and y_t^* are in quite good agreement with the renormalization predictions[63,53] $Q=8\pi^2/\Gamma^4(1/4)=0.456947\ldots$ and $y_t^*=d/2$. However, the uncertainties in the estimates increase considerably with increasing σ, because the leading irrelevant exponent becomes very small. An exception is the relatively large uncertainty in $y_t^*(d=1,\sigma=0.2)$, which originates from the fact that the Monte Carlo data were taken in a rather narrow temperature region around the critical point. Furthermore, an accurate simultaneous determination of Q and y_t^* is very difficult, because of the correlation between the two quantities. Therefore we have repeated the same analysis with Q fixed at its theoretical prediction—as appears justified by the values for Q in Table I—in order to obtain more accurate estimates for y_t^*. The results, shown in the fifth column of Table I, are indeed in good agreement with the theoretically expected values (last column). Thus, we have kept the thermal exponent fixed at its theoretical value in the further analysis, just as in Ref. 53. The corresponding results for Q and K_c are shown in Table II. As discussed in Ref. 53, over the full range of σ and d the Monte Carlo results for Q show good agreement with the renormalization prediction, thus confirming the universality of this quantity above the upper critical dimension. In comparison with the estimates presented in Table I of Ref. 53, some minor remarks apply. For $Q(d=3,\sigma=0.4)$ one decimal place too much was quoted, suggesting a too high accuracy. Furthermore we note that the newest result for $K_c(d=3,\sigma=1.2)$ deviates two standard deviations from the earlier estimate and that the accuracy of $Q(d=3,\sigma=1.4)$ is less than in Ref. 53. The latter difference is due to the fact that we have taken into account more corrections to scaling.

TABLE II. The amplitude ratio Q and critical couplings K_c for systems with long-range interactions in one, two, and three dimensions, for several values of the decay parameter $0<\sigma\leqslant d/2$. The thermal exponent (see Table I) was kept fixed at its theoretical value in all analyses. The estimates for K_c in the last column have been obtained by fixing Q at its renormalization prediction. The numbers between parentheses represent the errors in the last decimal places.

d	σ	Q	K_c	K_c
1	0.1	0.4565 (8)	0.0476162 (13)	0.0476168 (6)
1	0.2	0.4579 (7)	0.092234 (2)	0.0922314 (15)
1	0.25	0.4579 (15)	0.114143 (4)	0.1141417 (19)
1	0.3	0.4567 (15)	0.136113 (4)	0.136110 (2)
1	0.4	0.457 (3)	0.181151 (8)	0.181150 (3)
1	0.5	0.463 (5)	0.229157 (8)	0.229155 (6)
2	0.2	0.4573 (10)	0.028533 (3)	0.0285324 (14)
2	0.4	0.4565 (17)	0.051824 (4)	0.0518249 (14)
2	0.6	0.456 (4)	0.071364 (7)	0.071366 (2)
2	0.8	0.458 (5)	0.088094 (7)	0.088094 (2)
2	1.0	0.447 (8)	0.102556 (5)	0.102558 (5)
3	0.2	0.4584 (9)	0.0144361 (10)	0.0144354 (6)
3	0.4	0.4569 (8)	0.0262927 (16)	0.0262929 (7)
3	0.6	0.4581 (9)	0.036050 (2)	0.0360469 (11)
3	0.8	0.4562 (13)	0.044034 (2)	0.0440354 (10)
3	1.0	0.4571 (14)	0.050515 (2)	0.0505152 (12)
3	1.2	0.457 (3)	0.055682 (3)	0.0556825 (14)
3	1.4	0.455 (5)	0.059666 (2)	0.0596669 (11)
3	1.5	0.449 (7)	0.061251 (2)	0.061253 (2)

The universality of Q is illustrated graphically in Figs. 1(a)–1(c), where the increasing importance of corrections to scaling upon approaching the upper critical dimension clearly follows from the size of the error bars. At the upper critical dimension itself ($\varepsilon=0$) this culminates in the appearance of logarithmic corrections, where the finite-size scaling form of Q_L is given by

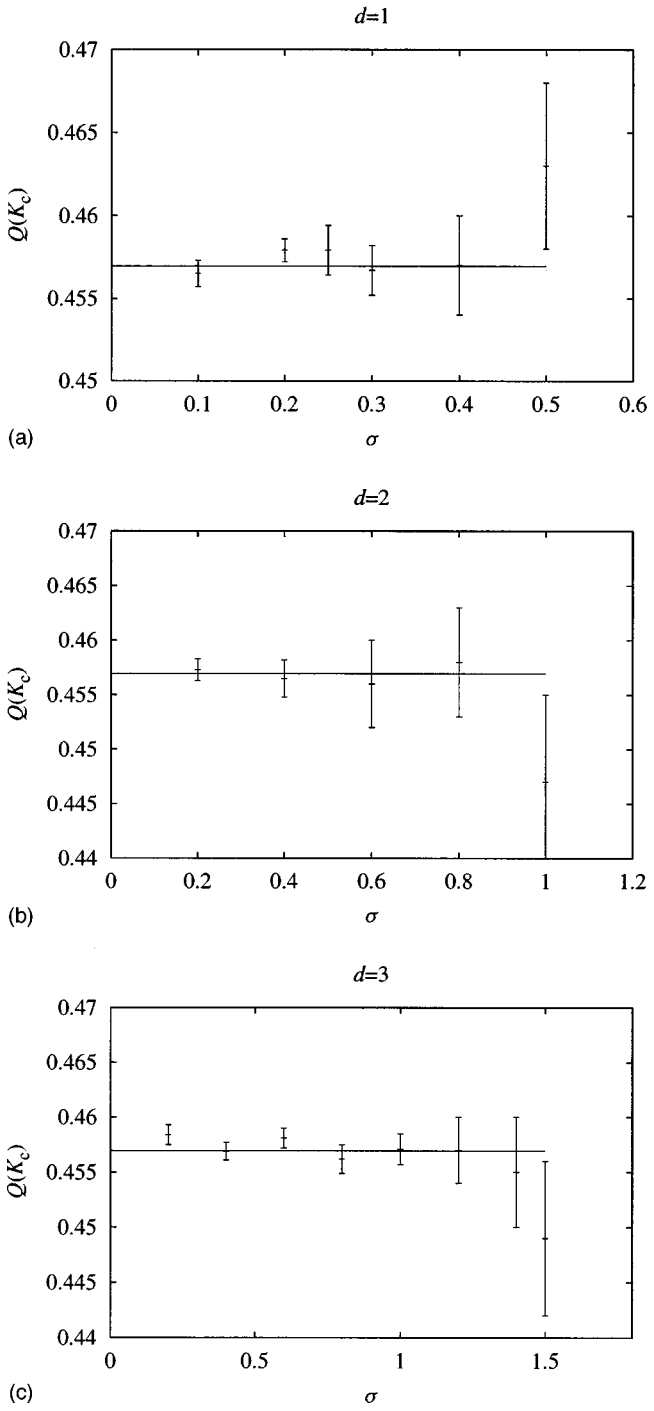

FIG. 1. The amplitude ratio Q as a function of the decay parameter σ in (a) $d=1$, (b) $d=2$, and (c) $d=3$ dimensions. The solid line marks the renormalization prediction.

$$Q_L(T)=Q+p_1L^{y_t}(\ln L)^{1/6}\left[t+v\frac{L^{-y_t}}{(\ln L)^{2/3}}\right]+p_2L^{2y_t}(\ln L)^{1/3}\times\left[t+v\frac{L^{-y_t}}{(\ln L)^{2/3}}\right]^2+q_1L^{d-2y_h}+\cdots+\frac{q_3}{\ln L}+\cdots. \tag{20}$$

The ellipses denote terms containing higher powers of L^{d-2y_h} and $1/\ln L$. The extremely slow convergence of this series is reflected in the uncertainty in the resulting estimates for Q at the upper critical dimension. To illustrate the dependence of the finite-size corrections on ε more directly, Fig. 2(a) displays (for various values of σ) the finite-size scaling functions as they follow from a least-squares fit of the data for $d=1$ to Eqs. (19) and (20), respectively. Although one clearly observes the increase of finite-size corrections when $\sigma\to d/2$, the true nature of the logarithmic corrections in Eq. (20) cannot be appreciated from this graph. To emphasize the difference between $\varepsilon=0$ and $\varepsilon<0$, we therefore also show [Fig. 2(b)] the same plot for the enormous range $0<L<10^{10}$. Now it is evident how strongly the case $\varepsilon=0$ differs even from a case with strong power-law corrections, such as $\sigma=0.4$ ($\varepsilon=-0.2$).

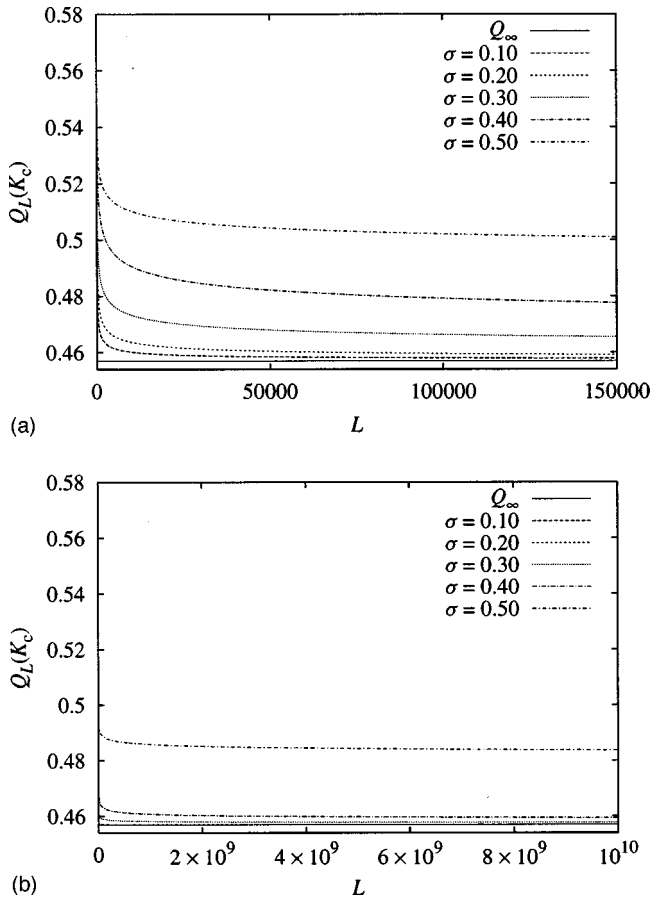

FIG. 2. The amplitude ratio Q in a one-dimensional system as a function of the system size L for various values of σ. (a) illustrates the increase of the finite-size corrections when the upper critical dimension ($\sigma=d/2$) is approached. (b) emphasizes the difference between finite-size corrections *above* the upper critical dimension (power-law) and at the upper critical dimension itself (logarithmic).

We have used the universality of Q to considerably narrow the error margins on K_c by fixing Q at its theoretical value in the least-squares fit. The corresponding couplings are shown in Table II as well. The relative accuracy of the critical couplings lies between 1.5×10^{-5} and 5.0×10^{-5}. For the one-dimensional case, we can compare these results to earlier estimates, see Table III. One notes that the newest estimates are more than two orders of magnitude more accurate than previous estimates. The first estimates[18] were obtained by carrying out exact calculations for chains of 1 to 20

TABLE III. Comparison between our best estimates of the critical couplings K_c for the one-dimensional system and earlier estimates.

σ	This work	Ref. 18	Ref. 19	Ref. 20	Ref. 42	Ref. 21	Ref. 27	Ref. 43
0.1	0.0476168 (6)		0.0478468	0.0505 (5)	0.04635	0.04777 (12)	0.0469	0.0481
0.2	0.0922314 (15)	0.0926 (5)	0.0933992	0.0923 (9)	0.09155	0.0928 (3)	0.0898	
0.25	0.1141417 (19)						0.1106	
0.3	0.136110 (2)	0.1370 (7)	0.138478	0.1362 (14)	0.1359	0.1375 (10)	0.1314	0.144
0.4	0.181150 (3)	0.1825 (10)	0.184081	0.1815 (18)	0.1813	0.183 (2)	0.1750	
0.5	0.229155 (6)	0.2307 (14)	0.230821	0.230 (2)	0.2295	0.231 (4)	0.2251	0.250

spins and subsequently extrapolating these results using Padé approximants. Note that the estimates for T_c in Ref. 18 are expressed in units of the inverse of the Riemann zeta function and thus must be multiplied by $\zeta(1+\sigma)$. All couplings are somewhat too high, but still in fair agreement with our estimates. The results of Doman[19] have no error bars. Still, his results concern us, since he carries out a cluster approach, obtaining critical couplings which start at the mean-field value for cluster size zero and increase monotonically with increasing cluster size, as they should, since mean-field theory yields a lower bound on the critical couplings (see below). Thus, he argues that the true couplings will lie *higher* than his best estimates (obtained for cluster size 10). However, all these best estimates lie already *above* our estimates, which seems to indicate a problem inherent in his approach. Reference 20 presents results of an approximation coined ''finite-range scaling'' with error margins of 1%. For $\sigma=0.1$ the error is considerably underestimated, but for the other values of the decay parameter the couplings agree with our results well within the quoted errors. The same technique was applied in Ref. 42, but now the uncertainty in the couplings was estimated to be less than 10%, for small σ a few times larger. This is clearly a too conservative estimate, as the difference with our results is only a few percent for $\sigma=0.1$ and considerably less for larger σ. In Ref. 21, the coherent-anomaly method was used to obtain two different estimates without error margins. We have quoted the average of the two results, with their difference as a crude measure for the uncertainty. The agreement is quite good, although all results lie systematically above our values. Yet another approach has been formulated in Ref. 27, where the Onsager reaction-field theory was applied to obtain a general expression for the critical coupling,

$$K_c(\sigma)=\frac{\Gamma(1+\sigma)\sin(\pi\sigma/2)}{(1-\sigma)\pi^{1+\sigma}}. \tag{21}$$

Unfortunately, no estimate for the accuracy of this expression is given, but it seems to generally underestimate the critical coupling by a few percent. Finally, some estimates have recently been obtained by means of the real-space renormalization-group technique.[43]

In addition, Monroe has calculated various bounds on the critical couplings as shown in Table IV. The Bethe lattice approximation[24] was used to obtain both upper and lower bounds, to which our results indeed conform, although it must be said that the upper bounds do not constitute a very stringent criterion. Furthermore, the application of Vigfusson's method[25] has yielded even closer lower bounds for $\sigma=0.1$ and $\sigma=0.2$.

Apart from these approximations, one may also use mean-field theory to make some predictions concerning the critical coupling in the limit $\sigma\downarrow 0$. It was shown by Brankov[64] that in this limit the d-dimensional system with an interaction potential $\propto\sigma/r^{d+\sigma}$ is equivalent to the Husimi-Temperley mean spherical model. More specifically, it was conjectured by Cannas[26] that for the one-dimensional case $\lim_{\sigma\to 0}K_c\sim\sigma/2$, which is also the first term in the Taylor expansion of Eq. (21). Indeed, in mean-field theory one has $zK_c^{\mathrm{MF}}=1$, where z is the coordination number. For $d=1$ this corresponds to the requirement

$$2K_c^{\mathrm{MF}}(\sigma)\sum_{n=1}^{\infty}\frac{1}{n^{1+\sigma}}=2K_c^{\mathrm{MF}}(\sigma)\zeta(1+\sigma)=1, \tag{22}$$

where $\zeta(x)$ denotes the Riemann zeta function. The expansion of $\zeta(x)$ around $x=1$ yields the conjectured relation $\lim_{\sigma\downarrow 0}K_c^{\mathrm{MF}}=\sigma/2$. Figure 3(a) shows the critical coupling as a function of the decay parameter σ along with $K_c^{\mathrm{MF}}(\sigma)$ and the asymptotic behavior for $\sigma\downarrow 0$. One observes that $K_c(\sigma)$ indeed approaches $K_c^{\mathrm{MF}}(\sigma)$ when σ approaches zero. Furthermore, $K_c^{\mathrm{MF}}(\sigma)$ is smaller than $K_c(\sigma)$ for all σ, as one expects from the fact that mean-field theory *over*estimates the critical temperature. It is interesting to note that for $\sigma=0.1$ ($K_c^{\mathrm{MF}}\approx 0.047239$) this lower bound already excludes the estimates given in Refs. 42 and 27 (cf. Table III). Replacing zK_c^{MF} by the integrated interaction, we can generalize such estimates to higher dimensionalities,

$$K_c^{\mathrm{MF}}(\sigma)\frac{2\pi^{d/2}}{\Gamma\left(\frac{d}{2}\right)}\int_{m_0}^{\infty}dr\,\frac{1}{r^{1+\sigma}}=1. \tag{23}$$

TABLE IV. Comparison of our best estimates of the critical couplings for the one-dimensional system with some lower and upper bounds.

σ	This work	Ref. 24	Ref. 24	Ref. 25
0.1	0.0476168 (6)	$\geqslant$0.04726	$\leqslant$0.09456	$\geqslant$0.04753
0.2	0.0922314 (15)	$\geqslant$0.08947	$\leqslant$0.1792	$\geqslant$0.09162
0.3	0.136110 (2)	$\geqslant$0.1273	$\leqslant$0.2558	
0.4	0.181150 (3)	$\geqslant$0.1615	$\leqslant$0.3258	
0.5	0.229155 (6)	$\geqslant$0.1923	$\leqslant$0.3903	—

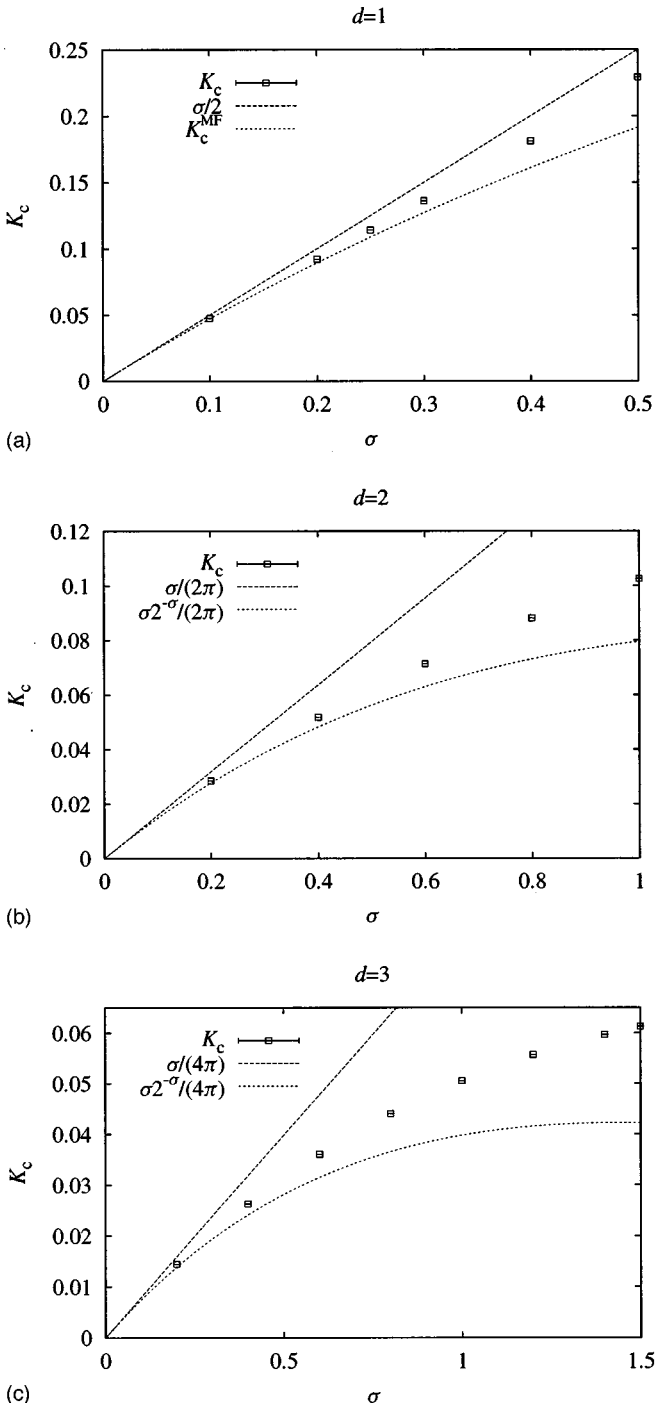

FIG. 3. The critical coupling K_c as a function of the decay parameter σ for (a) $d=1$, (b) $d=2$, and (c) $d=3$. Also shown is the asymptotic behavior for $\sigma \downarrow 0$ as predicted by mean-field theory and mean-field values for K_c over the full range of $0<\sigma<d/2$ (for $d=2$ and $d=3$ only approximately).

For $d>1$, the lower distance cutoff m_0 of the integral, i.e., the minimal interaction distance with the nearest neighbors, does not have an isotropic value, since there is no interaction within an elementary *cube* around the origin. Nevertheless, a constant value m_0, e.g., $m_0=1/2$, is a good approximation. Furthermore, for $d=1$ the integral is only a first-order approximation of Eq. (22), but for $d=2$ and $d=3$ it precisely corresponds to the interaction (18) and its generalization to $d=3$, respectively. As a first estimate one thus obtains

$$\lim_{\sigma \downarrow 0} K_c^{\mathrm{MF}}(\sigma)=\frac{\Gamma(d/2)}{2\pi^{d/2}}\sigma m_0^{\sigma}. \tag{24}$$

An expansion in terms of σ shows that the first term is independent of m_0. For $d=1,2,3$ one finds, respectively, $K_c^{\mathrm{MF}}\sim\sigma/2$, $K_c^{\mathrm{MF}}\sim\sigma/(2\pi)$, $K_c^{\mathrm{MF}}\sim\sigma/(4\pi)$. Figures 3(b) and 3(c) show $K_c(\sigma)$ for $d=2$ and $d=3$, the corresponding asymptotes and Eq. (24) with $m_0=1/2$.

The deviation of $K_c(\sigma)$ from $K_c^{\mathrm{MF}}(\sigma)$ is also expressed by the last term in the renormalization expression (6). However, in order to assess the σ dependence of this term one has to calculate the σ dependence of the coefficients a and c, arising from the integrals over the σ-dependent propagators.

C. Determination of critical exponents

1. Magnetic susceptibility

The magnetic susceptibility χ is directly proportional to the average square magnetization density,

$$\chi=L^d\langle m^2\rangle, \tag{25}$$

and thus we can use Eq. (14) to analyze the finite-size data. Expanding this equation in t and u we obtain for $\varepsilon<0$

$$\chi=L^{2y_h^*-d}(a_0+a_1\hat{t}L^{y_t^*}+a_2\hat{t}^2L^{2y_t^*}+\cdots+b_1L^{y_i}+\cdots), \tag{26}$$

and for $\varepsilon=0$

$$\chi=L^{2y_h-d}\sqrt{\ln L}\left[a_0+a_1L^{y_t}(\ln L)^{1/6}\left(t+v\frac{L^{-y_t}}{(\ln L)^{2/3}}\right)+a_2L^{2y_t}(\ln L)^{1/3}\left(t+v\frac{L^{-y_t}}{(\ln L)^{2/3}}\right)^2+\cdots+\frac{b_1}{\ln L}+\cdots\right]. \tag{27}$$

The analytic part of the free energy might give rise to an additional constant, but this could not be observed in our simulations, because it is dominated by the corrections to scaling. In Table V we list the results of an analysis of the numerical data. For all examined systems we have determined the exponent y_h^* and the critical coupling. The estimates for the latter are in good agreement with those obtained from the analysis of the universal amplitude ratio Q. Furthermore, the exponents agree nicely, for all dimensionalities, with the renormalization prediction $y_h^*=3d/4$. Just as before, the uncertainties increase with increasing σ, although the analyses at the upper critical dimension itself seem to yield better results than those just above it. Compare in particular the results for $\sigma=1.4$ ($y_i=-0.2$) and $\sigma=1.5$. The logarithmic prefactor in Eq. (27) can be clearly observed in the sense that the quality of the least-squares fit decreases considerably when this factor is omitted. To reduce the uncertainty in the exponents we have repeated the analysis with K_c fixed at the best values in Table II, i.e., those obtained with fixed Q. The corresponding estimates of y_h^* are also shown in Table V and are indeed in good agreement with the renormalization predictions.

Now we can calculate the critical exponents and compare them to earlier estimates for $d=1$. We do this for the corre-

TABLE V. Estimates for the critical coupling K_c and the exponent y_h^* as obtained from the analysis of the magnetic susceptibility. The values for y_h^* in the fifth column have been obtained by fixing K_c at their best estimates from Table II; the error margins do not include the uncertainty in these values for K_c.

d	σ	K_c	y_h^*	y_h^*	RG
1	0.1	0.0476161 (19)	0.7487 (14)	0.7493 (6)	$\frac{3}{4}$
1	0.2	0.092239 (4)	0.752 (2)	0.7504 (10)	$\frac{3}{4}$
1	0.25	0.114145 (4)	0.7477 (15)	0.7468 (16)	$\frac{3}{4}$
1	0.3	0.136110 (5)	0.747 (3)	0.7490 (17)	$\frac{3}{4}$
1	0.4	0.181170 (10)	0.749 (5)	0.746 (3)	$\frac{3}{4}$
1	0.5	0.229153 (6)	0.748 (2)	0.7490 (8)	$\frac{3}{4}$
2	0.2	0.028537 (5)	1.500 (6)	1.495 (3)	$\frac{3}{2}$
2	0.4	0.051830 (6)	1.498 (9)	1.496 (3)	$\frac{3}{2}$
2	0.6	0.071370 (5)	1.497 (6)	1.498 (2)	$\frac{3}{2}$
2	0.8	0.088095 (10)	1.496 (5)	1.495 (3)	$\frac{3}{2}$
2	1.0	0.102556 (3)	1.495 (4)	1.497 (2)	$\frac{3}{2}$
3	0.2	0.0144347 (9)	2.249 (2)	2.2504 (8)	$\frac{9}{4}$
3	0.4	0.026296 (2)	2.250 (6)	2.246 (3)	$\frac{9}{4}$
3	0.6	0.036046 (3)	2.246 (7)	2.244 (5)	$\frac{9}{4}$
3	0.8	0.0440349 (17)	2.243 (4)	2.246 (3)	$\frac{9}{4}$
3	1.0	0.050516 (3)	2.239 (9)	2.243 (7)	$\frac{9}{4}$
3	1.2	0.055679 (2)	2.247 (11)	2.251 (7)	$\frac{9}{4}$
3	1.4	0.0596636 (18)	2.27 (3)	2.26 (2)	$\frac{9}{4}$
3	1.5	0.061251 (2)	2.257 (12)	2.249 (5)	$\frac{9}{4}$

lation length exponent $\nu = 1/(y_t^* + y_i/2)$ and the magnetization exponent $\beta = (d - y_h^*)/y_t^*$. The results are shown in Tables VI and VII. Since all our estimates for y_t^* and y_h^* agree with the renormalization values, also ν and β are in agreement with the classical critical exponents. Unfortunately, the accuracy in both exponents is seriously hampered by the uncertainty in y_t^*, which has only been determined from the temperature-dependent term in Q. In particular the results for ν from Ref. 42 are, for small σ, in better agreement with the theoretically predicted values than our estimates. However, all previous results, both for ν and for β, deviate seriously from the predicted values when σ approaches 1/2, which is not the case for our values. This can probably be attributed to the fact that corrections to scaling have been taken into account more adequately.

2. Spin-spin correlation function

In Sec. III two different decay modes for the spin-spin correlation function were derived. The relative magnitude of r and L determines which of the modes applies. In the bulk of our simulations we have restricted r in $g(\mathbf{r})$ to $r = L/2$. Since this quantity reflects the $\mathbf{k} = \mathbf{0}$ mode of the correlation function, we write for $\varepsilon < 0$ an expression analogous to that for the magnetic susceptibility,

$$g(L/2) = L^{2y_h^* - 2d}[c_0 + c_1 \hat{t} L^{y_t^*} + c_2 \hat{t}^2 L^{2y_t^*} + \cdots + d_1 L^{y_i} + \cdots] \tag{28}$$

and for $\varepsilon = 0$

$$g(L/2) = L^{2y_h - 2d}\sqrt{\ln L}\left[c_0 + c_1 L^{y_t}(\ln L)^{1/6}\left(t + v\frac{L^{-y_t}}{(\ln L)^{2/3}}\right) + c_2 L^{2y_t}(\ln L)^{1/3}\left(t + v\frac{L^{-y_t}}{(\ln L)^{2/3}}\right)^2 + \cdots + \frac{d_1}{\ln L} + \cdots\right]. \tag{29}$$

For values of r such that $g(\mathbf{r})$ does *not* correspond to this mode of the correlation function, the σ-dependent exponent y_h will appear in Eq. (28) instead of y_h^*. Furthermore, the logarithmic prefactor in Eq. (29) will be absent, as it arises from the dangerous irrelevant variable [cf. Eq. (15)]. The results of our analysis are shown in Table VIII. They evidently corroborate that the exponent y_h^* coincides with that appearing in the susceptibility. Also the factor $\sqrt{\ln L}$ in Eq. (29) was clearly visible in the least-squares analysis. The critical couplings agree with the estimates from Q and χ and we have again tried to increase the accuracy in y_h^* by repeating the analysis with K_c fixed at their best values in Table II. The accuracy of the results is somewhat less than of those obtained from the magnetic susceptibility, because we have now only used numerical data for even system sizes. The fact that the L dependence of $g(L/2)$ is determined by the $\mathbf{k} = \mathbf{0}$ mode raises the question whether one can also observe the power-law decay described by η in finite systems. To this end, we have sampled $g(r)$ as a function of r in the one-dimensional model. In order to clearly distinguish the two predictions for the decay of $g(r)$ we have examined a system far from the upper critical dimension, viz., with $\sigma = 0.1$. It turned out to be necessary to sample *very* large system sizes to observe the regime where $g(r) \propto r^{-(d-\sigma)}$. Figure 4 displays the spin-spin correlation function scaled with $L^{d/2}$ versus r/L. The scaling makes the results collapse for r of the

TABLE VI. The correlation length exponent ν as a function of σ for the one-dimensional model, together with earlier estimates and the renormalization predictions.

σ	This work	Ref. 20	Ref. 42	Ref. 43	RG
0.1	9.3 (6)	9.12	9.9	10.48	10.0
0.2	4.9 (3)	4.90	4.95		5.0
0.25	4.00 (8)				4.0
0.3	3.27 (12)	3.41	3.32	3.90	3.3...
0.4	2.50 (13)	2.71	2.68		2.5
0.5	2.04 (8)	2.34	2.33	2.81	2.0

TABLE VII. The magnetization exponent β as a function of σ for the one-dimensional model, together with earlier estimates and the renormalization predictions.

σ	This work	Ref. 18	Ref. 21	RG
0.1	0.494 (8)		0.495	$\frac{1}{2}$
0.2	0.495 (13)	0.5	0.482	$\frac{1}{2}$
0.25	0.506 (8)			$\frac{1}{2}$
0.3	0.497 (15)	0.48	0.460	$\frac{1}{2}$
0.4	0.51 (2)	0.45	0.435	$\frac{1}{2}$
0.5	0.51 (2)	0.39	0.408	$\frac{1}{2}$

TABLE VIII. Estimates for the critical coupling K_c and the exponent y_h^* as obtained from the analysis of the spin-spin correlation function. The values for y_h^* in the fifth column have been obtained by fixing K_c at their best estimates from Table II; the error margins do not include the uncertainty in these values for K_c.

d	σ	K_c	y_h^*	y_h^*	RG
1	0.1	0.047619 (3)	0.750 (2)	0.7488 (9)	$\frac{3}{4}$
1	0.2	0.092233 (7)	0.749 (3)	0.7513 (16)	$\frac{3}{4}$
1	0.25	0.114148 (10)	0.750 (5)	0.747 (2)	$\frac{3}{4}$
1	0.3	0.136116 (7)	0.753 (5)	0.752 (3)	$\frac{3}{4}$
1	0.4	0.181158 (15)	0.747 (7)	0.750 (4)	$\frac{3}{4}$
1	0.5	0.229150 (7)	0.749 (2)	0.7503 (10)	$\frac{3}{4}$
2	0.2	0.028535 (7)	1.499 (9)	1.496 (3)	$\frac{3}{2}$
2	0.4	0.051831 (6)	1.505 (6)	1.499 (4)	$\frac{3}{2}$
2	0.6	0.071369 (6)	1.507 (4)	1.502 (4)	$\frac{3}{2}$
2	0.8	0.088091 (6)	1.495 (7)	1.497 (3)	$\frac{3}{2}$
2	1.0	0.102554 (4)	1.490 (6)	1.496 (3)	$\frac{3}{2}$
3	0.2	0.0144348 (16)	2.256 (6)	2.254 (4)	$\frac{9}{4}$
3	0.4	0.026296 (3)	2.257 (8)	2.245 (5)	$\frac{9}{4}$
3	0.6	0.036053 (4)	2.262 (10)	2.246 (4)	$\frac{9}{4}$
3	0.8	0.044035 (4)	2.252 (11)	2.250 (5)	$\frac{9}{4}$
3	1.0	0.050511 (5)	2.228 (15)	2.249 (9)	$\frac{9}{4}$
3	1.2	0.055680 (3)	2.253 (14)	2.257 (9)	$\frac{9}{4}$
3	1.4	0.059667 (2)	2.22 (4)	2.31 (4)	$\frac{9}{4}$
3	1.5	0.061251 (5)	2.26 (3)	2.248 (7)	$\frac{9}{4}$

order of the system size. Here, the correlation function levels off. This is the mean-field like contribution to the correlation function, which dominates in the spatial integral yielding the magnetic susceptibility. For small r the data do not collapse at all, which shows that $g(r)$ exhibits different scaling behavior in this regime. Indeed, the correlation function decays here as $r^{-(d-\sigma)}=r^{-0.9}$ and not as $r^{-d/2}$. Note, however, that this regime is restricted to a small region of r and can only be observed for very large system sizes.

It is interesting to note that already Nagle and Bonner[18] have tried to calculate η in a spin chain with long-range interactions from finite-size data for the susceptibility. Because this calculation relied on the assumption that $\chi(L,K_c)-\chi(L-1,K_c)\sim g(L)\sim L^{-(d-2+\eta)}$, they called the corresponding exponent $\tilde{\eta}$. The results for $\tilde{\eta}$ turned out to assume a constant value approximately equal to 1.50 for $0<\sigma\leqslant 0.5$. Thus, the identification of $\tilde{\eta}$ with η was assumed to be invalid in Ref. 35. Now we see that $\tilde{\eta}$ is in excellent agreement with $\eta^*\equiv d+2-2y_h^*=2-d/2$.

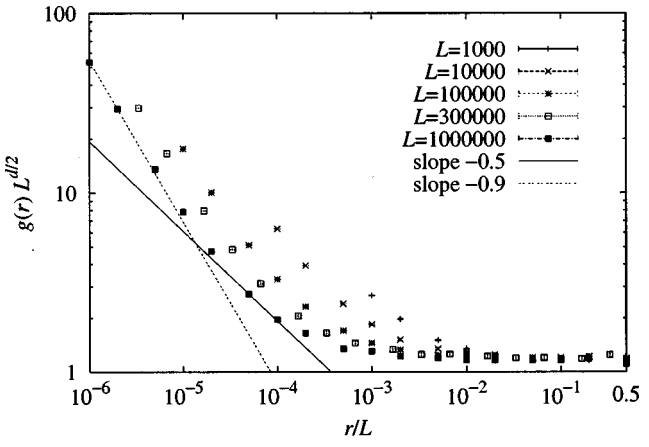

FIG. 4. The spin-spin correlation function versus r/L in the one-dimensional model with $\sigma=0.1$. Results for various system sizes are shown. For a discussion see the text.

V. CONCLUSIONS

In this paper we have studied systems with long-range interactions decaying as $r^{-(d+\sigma)}$ in one, two, and three dimensions in the regime where these interactions exhibit classical critical behavior, i.e., for $0<\sigma\leqslant d/2$. From the renormalization equations we have derived the scaling behavior, including the corrections to scaling, for various quantities. These predictions, in particular the critical exponents and the scaling behavior of the amplitude ratio $\langle m^2\rangle^2/\langle m^4\rangle$, have been verified by accurate Monte Carlo results. At the upper critical dimension, the logarithmic factors appearing in the finite-size scaling functions could be accurately observed. The Monte Carlo results have been obtained with a dedicated algorithm. This algorithm is many orders of magnitude faster (up to the order of 10^8 for the largest examined system) than a conventional Monte Carlo algorithm for these systems. Our analysis has also yielded estimates for the critical couplings. For $d=1$ these values have an accuracy which is more than two orders of magnitude better than previous estimates and could thus serve as a check for half a dozen different approximations. For $d=2$ and $d=3$ we have, to our best knowledge, obtained the first estimates for the critical couplings. Finally, we have given both theoretical and numerical arguments that above the upper critical dimension the decay of the critical spin-spin correlation function in finite systems consists of two regimes: One where it decays as $r^{-(d-2+\eta)}$ and one where it is independent of the distance.

As an outlook we note that many interesting results may be expected *below* the upper critical dimension, where neither any rigorous results nor any accurate numerical results are available. This regime will be the subject of a future investigation.[58]

APPENDIX: DETAILS OF THE MONTE CARLO ALGORITHM FOR LONG-RANGE INTERACTIONS

The cluster algorithm applied in this study has been described for the first time in Ref. 54. A somewhat more elaborate treatment of the mathematical aspects was given in Ref. 65. Although conceptually no new aspects arise in the application to algebraically decaying interactions in more than one dimension, several important practical issues must be taken care of in actual simulations. It is the purpose of this appendix to discuss these issues and their solutions in some more detail. We do not repeat the full cluster algorithm here, but only describe how the cluster formation process proceeds from a given spin s_i which has already been added to the cluster (the so-called *current* spin).

As explained in Ref. 54, the key element of the algorithm lies in splitting up the so-called bond-activation probability $p(s_i,s_j)=\delta_{s_i s_j}\,p_{ij}=\delta_{s_i s_j}[1-\exp(-2J_{ij})]$ into two parts,

namely the Kronecker delta testing whether the spins s_i and s_j are parallel and the ''provisional'' bond-activation probability p_{ij}. This enables us to define a *cumulative bond probability* $C(k)$, from which we can read off which bond is the next one to be provisionally activated

$$C(j) \equiv \sum_{n=1}^{j} P(n) \tag{A1}$$

with

$$P(n) = (1-p_1)(1-p_2)\cdots(1-p_{n-1})p_n . \tag{A2}$$

$p_j \equiv 1-\exp(-2J_j)$ is an abbreviation for p_{0j}, i.e., we define the origin at the position of the current spin. When comparing the expressions to those in Ref. 54 one must take into account that we now are working with Ising instead of Potts couplings. $P(n)$ is the probability that in the first step $n-1$ bonds are skipped and the nth bond is provisionally activated. Now the next bond j that is provisionally activated is determined by a random number $g \in [0,1\rangle$: $j-1$ bonds are skipped if $C(j-1) \leqslant g < C(j)$. The number j can be easily determined from g once we have tabulated the quantity $C(j)$ in a lookup table. If the jth bond is placed to a spin s_j that is indeed parallel to the current spin s_i then s_j is added to the cluster (i.e., the jth bond is activated). Subsequently we skip again a number of bonds before another bond at a distance $k>j$ is provisionally activated. The appropriate cumulative probability is now given by a generalization of Eq. (A1) (see Ref. 54),

$$\begin{aligned} C_j(k) &= \sum_{n=j+1}^{k} \left[\prod_{m=j+1}^{n-1} (1-p_m) \right] p_n \\ &= 1-\exp\left(-2 \sum_{n=j+1}^{k} J_n \right). \end{aligned} \tag{A3}$$

In principle we need now for each value of j another lookup table containing the $C_j(k)$. This is hardly feasible and fortunately not necessary, as follows from a comparison of Eqs. (A1) and (A3). Namely,

$$\begin{aligned} C(k) = C_0(k) &= C(j) + \left[\prod_{i=1}^{j} (1-p_i) \right] C_j(k) \\ &= C(j) + [1-C(j)]C_j(k) \end{aligned} \tag{A4}$$

or $C_j(k) = [C(k)-C(j)]/[1-C(j)]$. So we can calculate $C_j(k)$ directly from $C(k)$. In practice one realizes this by using the bond distance j of the previous bond that was provisionally activated to rescale the (new) random number g to $g' \in [C(j),1\rangle$; $g' = C(j) + [1-C(j)]g$. Since we consider only ferromagnetic interactions, $\lim_{j\to\infty} C(j)$ exists and is smaller than 1, cf. Eq. (A3). Still we can accommodate only a limited number of bond distances in our lookup table and must therefore devise some approximation scheme to handle the tail of the long-range interaction, which is essential for the critical behavior. This issue is addressed below. Furthermore, this description only takes into account the bonds placed in one direction. The actual implementation of the algorithm must of course allow for bonds in both directions (assuming that $d=1$).

An alternative for the lookup table exists for interactions which can be explicitly summed. In those cases, Eq. (A3) can be solved for k, yielding an expression for the bond distance in terms of $C_j(k)$, i.e., in terms of the random number g. For the interaction defined in Sec. II the sum appearing in the right-hand side of Eq. (A3) is (for $j=0$) the truncated Riemann zeta function,

$$\sum_{n=1}^{k} J_n = K \sum_{n=1}^{k} \frac{1}{n^{d+\sigma}}, \tag{A5}$$

which cannot be expressed in closed form. In more than one dimension, a lookup table is very impractical and an interaction which *can* be summed explicitly becomes very desirable. Therefore we have taken an isotropic, continuous interaction of the form $J = K/r^{d+\sigma}$. The interaction with a spin at lattice site $\mathbf{n}$ is then given by the integral of J over the elementary square (cube) centered around $\mathbf{n}$ [cf. Eq. (18)] and the cumulative bond probability yields the (not necessarily integer-valued) distance k at which the first provisional bond is placed. To this end, the sum in Eq. (A3) is replaced by a d-dimensional integral over the coupling J. As J is isotropic, only an integral over the radius remains, which runs from the minimal bond distance up to k. Thus for $d=2$ Eq. (A3) reduces to

$$C_j(k) = 1-\exp\left[-2\frac{2\pi K}{\sigma}\left(\frac{1}{j^\sigma} - \frac{1}{r^\sigma} \right) \right] \tag{A6}$$

and in $d=3$ the factor 2π is simply replaced by 4π. Equating $C_j(k)$ to the random number g we find

$$k = \left[j^{-\sigma} + \frac{\sigma}{4\pi K} \ln(1-g) \right]^{-1/\sigma}. \tag{A7}$$

Rescaling of the random number is no longer required: The lowest value, $g=0$, leads to a provisional bond at the same distance as the previous one, $k=j$. If $g = C_j(\infty) = 1-\exp[-(4\pi K/\sigma)j^{-\sigma}]$ the next provisional bond lies at infinity and thus $g \in [C_j(\infty),1\rangle$ yields no bond at all. Once the distance k has been obtained, $d-1$ further random numbers $g_1, g_2, \ldots$ are required to determine the *direction* of the bond. In $d=2$, we set $\phi = g_1/(2\pi)$. The coordinates of the next provisional bond (relative to the current spin) are then $(r_x, r_y) = (k\cos\phi, k\sin\phi)$, which are rounded to the nearest integer coordinates. Finally, the periodic boundary conditions are applied to map these coordinates onto a lattice site. For the next provisional bond, j is set equal to k (*not* to the rounded distance) and a new k is determined. If no bond has been placed yet, j is set to 1/2, the lowest possible bond distance. Hence it is possible to find a $1/2 \leqslant k < \sqrt{2}/2$ and an angle ϕ such that the corresponding lattice site is the origin. This does not affect the bond probabilities, but it is of course a ''wasted'' Monte Carlo step. For $d=3$ the process is similar, except that we need another random number g_2 to determine a second angle $-\pi/2 < \psi \leqslant \pi/2$, such that $\sin\psi$ is distributed uniformly; $\sin\psi = 1-2g_2$. The bond coordinates are given by $(k\cos\psi\cos\phi, k\cos\psi\sin\phi, k\sin\psi)$.

This approach can also be applied in the one-dimensional case, where the geometrical factor 2π in Eq. (A6) must be replaced by 2, which reflects the fact that bonds can be put to

the left and to the right of the origin. The direction of the bond is then simply determined by another random number. As has already been mentioned in Ref. 54, this can be used to cope with the limited size M of the lookup table. Beyond the bond distance M the sum in Eq. (A3) is approximated by an integral. I.e., if the random number g lies in the interval $[C(M),C(\infty)\rangle$, the bond distance k is determined from the one-dimensional version of Eq. (A7), where the lower part of the integral is replaced by an explicit sum

$$k=\left[\left(M+\frac{1}{2}\right)^{-\sigma}+\sigma\left(\frac{1}{2K}\ln(1-g)+\sum_{n=1}^{M}\frac{1}{n^{1+\sigma}}\right)\right]^{-1/\sigma}. \tag{A8}$$

Here, the geometrical factor is absent, as we have opted to treat ''left'' and ''right'' separately in our simulations (no additional random number is required in that case). The approximation (A8) effectively introduces a modification of the spin-spin interaction, which however can be made arbitrarily small by increasing M. Note that the offset 1/2 in the first term ensures a precise matching of the discrete sum and the integral approximation: the random number $g=C(M)=1-\exp[-2K\Sigma_{n=1}^{M}n^{-(1+\sigma)}]$ yields $k=M+1/2$ which is precisely the lowest k that is rounded to the integer bond distance $M+1$.

The accuracy of this procedure is further limited by the finite resolution of random numbers. For example, in our simulations the original random numbers are integers in the range $[0,2^{32}-1]$. Thus, for bond distances l such that $C(l)-C(l-1)$ is of the order 2^{-32}, the discreteness of the random numbers is no longer negligible. For $d=2$ and $d=3$, the discreteness of the angles also limits the lattice sites that can be selected for a provisional bond, but this generally occurs at distances larger than l. Once the value of l has been determined, with a safe margin, there are various approaches to this limitation. One may, e.g., draw another random number to determine the precise bond distance. A simpler approach is to distribute all bonds beyond l uniformly over the lattice, in order to prevent that certain lattice sites are never selected. However, one should take care that such simple approaches do not essentially modify the critical behavior. If l is relatively small, the error introduced by a random distribution of the bond distances might be larger than the effect of an interaction which decreases slightly nonmonotonically at large distances. Furthermore, in order to preserve the symmetry of the lattice, such a uniform distribution of the bonds should occur outside a square (cube) instead of a circle (sphere) with radius l.

*Electronic address: erik@tntnhb3.tn.tudelft.nl

[1] D. Ruelle, Commun. Math. Phys. **9**, 267 (1968).
[2] F. J. Dyson, Commun. Math. Phys. **12**, 91 (1969).
[3] F. J. Dyson, Commun. Math. Phys. **12**, 212 (1969).
[4] D. J. Thouless, Phys. Rev. **187**, 732 (1969).
[5] B. Simon and A. D. Sokal, J. Stat. Phys. **25**, 679 (1980).
[6] J. B. Rogers and C. J. Thompson, J. Stat. Phys. **25**, 669 (1981).
[7] J. Fröhlich and T. Spencer, Commun. Math. Phys. **84**, 87 (1982).
[8] J. Z. Imbrie, Commun. Math. Phys. **85**, 491 (1982).
[9] M. Aizenman, J. T. Chayes, L. Chayes, and C. M. Newman, J. Stat. Phys. **50**, 1 (1988).
[10] M. Aizenman and R. Fernández, Lett. Math. Phys. **16**, 39 (1988).
[11] J. Z. Imbrie and C. M. Newman, Commun. Math. Phys. **118**, 303 (1988).
[12] J. Bhattacharjee, S. Chakravarty, J. L. Richardson, and D. J. Scalapino, Phys. Rev. B **24**, 3862 (1981).
[13] G. V. Matvienko, Teor. Mat. Fiz. **63**, 465 (1985) [Theor. Math. Phys. **63**, 635 (1985)].
[14] B. Siu, J. Stat. Phys. **38**, 519 (1985).
[15] J. O. Vigfusson, Phys. Rev. B **34**, 3466 (1986).
[16] D. Rapaport and N. E. Frankel, Phys. Lett. **28A**, 405 (1968).
[17] J. F. Dobson, J. Math. Phys. (N.Y.) **10**, 40 (1969).
[18] J. F. Nagle and J. C. Bonner, J. Phys. C **3**, 352 (1970).
[19] B. G. S. Doman, Phys. Status Solidi B **103**, K169 (1981).
[20] Z. Glumac and K. Uzelac, J. Phys. A **22**, 4439 (1989).
[21] J. L. Monroe, R. Lucente, and J. P. Hourlland, J. Phys. A **23**, 2555 (1990).
[22] B. Bergersen and Z. Rácz, Phys. Rev. Lett. **67**, 3047 (1991).
[23] R. Mainieri, Phys. Rev. A **45**, 3580 (1992).
[24] J. L. Monroe, Phys. Lett. A **171**, 427 (1992).
[25] J. L. Monroe, J. Stat. Phys. **76**, 1505 (1994).
[26] S. A. Cannas, Phys. Rev. B **52**, 3034 (1995).
[27] A. S. T. Pires, Phys. Rev. B **53**, 5123 (1996).
[28] P. W. Anderson and G. Yuval, Phys. Rev. Lett. **23**, 89 (1969).
[29] G. Yuval and P. W. Anderson, Phys. Rev. B **1**, 1522 (1970).
[30] P. W. Anderson, G. Yuval, and D. R. Hamann, Phys. Rev. B **1**, 4464 (1970).
[31] P. W. Anderson and G. Yuval, J. Phys. C **4**, 607 (1971).
[32] J. M. Kosterlitz, Phys. Rev. Lett. **37**, 1577 (1976).
[33] J. L. Cardy, J. Phys. A **14**, 1407 (1981).
[34] S. A. Bulgadaev, Phys. Lett. **102A**, 260 (1984).
[35] M. E. Fisher, S.-k. Ma, and B. G. Nickel, Phys. Rev. Lett. **29**, 917 (1972).
[36] J. Sak, Phys. Rev. B **8**, 281 (1973).
[37] M. Suzuki, Y. Yamazaki, and G. Igarashi, Phys. Lett. **42A**, 313 (1972).
[38] G. Stell, Phys. Rev. B **1**, 2265 (1970).
[39] R. B. Griffiths, Phys. Rev. Lett. **24**, 1479 (1970).
[40] M. J. Wragg and G. A. Gehring, J. Phys. A **23**, 2157 (1990).
[41] H.-J. Xu, B. Bergersen, and Z. Rácz, Phys. Rev. E **47**, 1520 (1993).
[42] Z. Glumac and K. Uzelac, J. Phys. A **26**, 5267 (1993).
[43] S. A. Cannas and A. C. N. de Magalhães, J. Phys. A **30**, 3345 (1997).
[44] L. B. Bernardes and S. Goulart Rosa, Jr., Phys. Lett. A **191**, 193 (1994).
[45] J. M. Kosterlitz and D. J. Thouless, J. Phys. C **6**, 1181 (1973).
[46] J. M. Kosterlitz, J. Phys. C **7**, 1046 (1974).
[47] N. D. Mermin and H. Wagner, Phys. Rev. Lett. **17**, 1133 (1966).
[48] B. Hafskjold and G. Stell, in *The Liquid State of Matter: Fluids, Simple and Complex*, edited by E. W. Montroll and J. L. Lebowitz (North-Holland, Amsterdam, 1982), p. 175.
[49] M. E. Fisher, J. Stat. Phys. **75**, 1 (1994).
[50] R. Folk and G. Moser, Int. J. Thermophys. **16**, 1363 (1995).
[51] O. Boxberg and K. Westerholt, J. Magn. Magn. Mater. **140–144**, 1563 (1995).
[52] T. W. Burkhardt and E. Eisenriegler, Phys. Rev. Lett. **74**, 3189 (1995).

[53] E. Luijten and H. W. J. Blöte, Phys. Rev. Lett. **76**, 1557 (1996); **76**, 3662(E) (1996).
[54] E. Luijten and H. W. J. Blöte, Int. J. Mod. Phys. C **6**, 359 (1995).
[55] M. Kac and C. J. Thompson, J. Math. Phys. (N.Y.) **10**, 1373 (1969).
[56] L. D. Landau and E. M. Lifshitz, *Statistical Physics* (Pergamon, London, 1959).
[57] F. J. Dyson, Commun. Math. Phys. **21**, 269 (1971).
[58] E. Luijten and H. W. J. Blöte (unpublished).
[59] V. Privman and M. E. Fisher, J. Stat. Phys. **33**, 385 (1983).
[60] S.-k. Ma, *Modern Theory of Critical Phenomena* (Addison-Wesley, Redwood, California, 1976).
[61] K. Binder, Z. Phys. B **43**, 119 (1981).
[62] H. W. J. Blöte, E. Luijten, and J. R. Heringa, J. Phys. A **28**, 6289 (1995).
[63] E. Brézin and J. Zinn-Justin, Nucl. Phys. B **257** [FS14], 867 (1985).
[64] J. G. Brankov, Physica A **168**, 1035 (1990).
[65] E. Luijten, H. W. J. Blöte, and K. Binder, Phys. Rev. E **54**, 4626 (1996).